Revista de Chimie
https://revistadechimie.ro
https://doi.org/10.37358/Rev.Chim.1949

Reduction Characteristic of $CaSO_4$-CuO Combined Oxygen Carrier Under CO Atmosphere

KANG LI[1,2,3], MIN ZHENG[1,2,3*], JINGQUAN WANG[1,2,3], JUN WU[1,2,3]
[1] Faculty of Metallurgical and Energy, Kunming University of Science and Technology, Kunming 650093, China
[2] Power engineering, Kunming University of Science and Technology, Kunming 650093, China
[3] Engineering Research Center of Metallurgical Energy Conservation and Emission Reduction, Ministry of Education, Kunming University of Science and Technology, Kunming 650093, China

Abstract *$CaSO_4$ oxygen carrier is considered to be a potential oxygen carrier (OC) for Chemical Looping Combustion because of its high oxygen capacity and low price. But its reactivity is lower than the main metal oxide oxygen carriers, and it deactivates due to sulfur loss as well as sintering at high reaction temperatures above 920℃. To improve the performance of $CaSO_4$-based oxygen carrier, small amounts of CuO particles were mixed mechanistically with $CaSO_4$ particles to use as combined oxygen carrier in this work. The reduction reactions of $CaSO_4$ oxygen carrier, CuO oxygen carrier and $CaSO_4$-CuO combined oxygen carrier under CO atmosphere were investigated. The effects of reaction factors including reaction temperature, the oxygen-carrying ratio of CuO to $CaSO_4$ and mass of oxygen carrier, on the reductions have been investigated in this study. XRD, SEM-EDS, BET and gas analyses were performed to investigate the variations of solid phase, element compositions in solid residual and sulfur release with reaction time. The results show that the addition of CuO increases the reactivity of the CaSO4-based oxygen carrier while also suppressing the release of the gas sulfur. For the individual reduction of $CaSO_4$ by CO, with the increase of $CaSO_4$ mass (500 - 1200 mg), CO_2 yield also increases until 1000 mg stops and SO_2 released rises remarkably; An increase in the reaction temperature aggravated the SO_2 emission. The carbon dioxide generation efficiency also increases with an increase in temperature, but decreases when the temperature exceeds 950℃ due to sintering of the oxygen carrier particles; With respect to the reaction of CuO with CO, CO_2 yield does not change significantly with increasing temperature, due to the sintering of the CuO oxygen carrier in a high temperature reaction environment;For the combined oxygen carrier: a.As the reduction reaction temperature increases, the reduction reaction performance of the combined oxygen carrier is enhanced within the reaction temperature range of 750~900℃. b. CaO the use of CuO additives not only improves the CO conversion rate, but also inhibits the release of gas sulfide. As the oxygen carrying fraction of CuO increases, SO_2 released is reduced and the SO_2 release time is delayed. What' more, the solid products after reduction reaction mainly contain CaS, CaO, CuO, Cu_2O and $CaSO_4$, and no copper sulfide is detected. c. When the oxygen-carrying ratio of CuO to $CaSO_4$ is increasing from 15% to 20%, CO_2 yield increases greatly.*

Keywords: *Chemical Looping Combustion; Reduction reaction; CO_2 capture; $CaSO_4$ oxygen carrier; CuO oxygen carrier, SO_2 release*

1. Introduction

As CO_2 is one of the main components of greenhouse gases, it is urgent to reduce its emissions. Chemical-looping combustion (CLC) is different from traditional combustion. It uses oxygen atoms in the oxygen carrier to carry out a combustion reaction with the fuel, and only CO_2 and H_2O are produced in the combustion product. A high concentration of CO_2 can be obtained by simple condensation, thereby achieving energy-free capture of CO_2 [1,2]. In the CLC system, the performance of the oxygen carrier directly determines whether the Chemical-looping combustion technology can enter the practical application of industrialization [3].

**email: zhengmin1634@163.com*

At present, the study of oxygen carriers in the CLC is still mainly concentrated on metal oxide oxygen carriers, mainly including oxides of transition metals such as Ni [4-6], Fe [7-10], Cu [11,12], Co [13] and Mn [14-17] and their composite metal oxides. At the same time, extensive studies have been conducted on these metal oxygen carriers. The metal oxygen carrier has a high reaction rate and high temperature resistance. But their shortcomings are also obvious, such as expensive raw materials, heavy metal pollution and sulfur poisoning. For further large-scale commercial use, the low-cost materials also raise a growing concern.

$CaSO_4$ oxygen carrier has abundant reserves, low price and high oxygen carrier capacity (0.46) [18-20], so it has great potential for further large-scale commercial application of CLC.

Figure 1 shows a diagram of the CO-fueled CLC process based on $CaSO_4$ oxygen carrier. The general reaction method is as follows. In the fuel reactor, $CaSO_4$ is reduced to CaS by CO:

$$\frac{1}{4}\mathrm{CaSO_4} + \mathrm{CO} \rightarrow \frac{1}{4}\mathrm{CaS} + \mathrm{CO_2} \quad \Delta H^{\theta}_{298.15} = -42.76 kJ/mol \qquad \text{(R1)}$$

In the air reactor, the CaS is then oxidized by air into $CaSO_4$ and the molecular oxygen of O_2 in air is transferred to lattice oxygen in $CaSO_4$.

$$\mathrm{CaS} + 2\mathrm{O_2} \rightarrow \mathrm{CaSO_4} \quad \Delta H^{\theta}_{298.15} = -960.89 kJ/mol \qquad \text{(R2)}$$

In addition to the usual reactions, the following side reactions may occur:

$$\mathrm{CaSO_4}+\mathrm{CO}\rightarrow\mathrm{CaO}+\mathrm{CO_2}+\mathrm{SO_2} \quad \Delta H^{\theta}_{298.15}=219.19 kJ/mol \qquad \text{(R3)}$$
$$\mathrm{CaSO_4}+\mathrm{CO}\rightarrow\mathrm{CaCO_3}+\mathrm{SO_2} \quad \Delta H^{\theta}_{298.15}=40.39 kJ/mol \qquad \text{(R4)}$$
$$\frac{3}{4}\mathrm{CaSO_4}+\frac{1}{4}\mathrm{CaS}\rightarrow\mathrm{CaO}+\mathrm{SO_2} \quad \Delta H^{\theta}_{298.15}=261 kJ/mol \qquad \text{(R5)}$$
$$\mathrm{CaS}+3\mathrm{CO_2}\rightarrow\mathrm{CaO}+3\mathrm{CO}+\mathrm{SO_2} \quad \Delta H^{\theta}_{298.15} = 390.2 kJ/mol \qquad \text{(R6)}$$

As the above-mentioned side reactions, SO_2 gas is generated, and in addition, other sulfide gases are generated. This not only leads to a decrease in the oxygen capacity of $CaSO_4$ and reduces its reactivity, but also the release of the gas sulfur is extremely harmful to the environment.

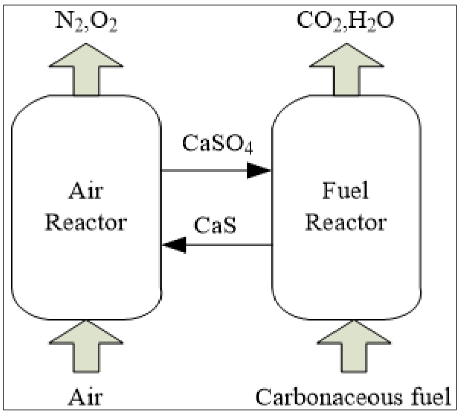

Figure 1. Schematic illustration of a chemical Looping combustion with a dual fluidized bed

In order to increase the reactivity of $CaSO_4$, an active transition metal oxide is added, and this has been studied intensively. Among them, there are many studies on Fe_2O_3. Due to the synergistic effect of $CaSO_4$ with the added Fe_2O_3, it was found that the reactivity of $CaSO_4$-Fe_2O_3 combined OC with gaseous fuel and different grades of coal was greatly improved [21,22]. In our previous studies, the addition of

CaO not only achieved high CO_2 production efficiency, but also inhibited the side reaction of $CaSO_4$ and prevented the emission of gaseous sulfur [23]. Wang et al. [24] reported to use the $CaSO_4$-CuO as an mixed OC for the coal-fueled CLC and confirmed its feasibility. They found that the reactivity of this mixed OC is greatly improved, and it has a good fixing ability to the sulfur produced from the side reaction of $CaSO_4$. Compared with Fe_2O_3, CuO has higher reactivity and its affinity capacity to sulfur is stronger. In addition, the reaction of CuO with fuel is an exothermic reaction. Therefore, CuO-$CaSO_4$ combined oxygen carrier should be a good choice to simultaneously promote the reactivity of $CaSO_4$ and inhibit gaseous sulfur emissions.

Herein, we report a OC by combining $CaSO_4$ and CuO to improve the performance of $CaSO_4$ as an oxygen carrier for CLC of CO. Experimental study on reduction reaction of $CaSO_4$-CuO combined oxygen carrier was undertaken in a small horizontal fixed reaction bed in this paper. The effects of reaction temperature, oxygen carrier mass, and oxygen carrying ratio of CuO to $CaSO_4$ on sulphur emission and CO_2 generation efficiency are taken into account. The results indicate that the addition of the CuO additive increases the reactivity of the calcium-based oxygen carrier while suppressing the release of the sulfurized gas.

2. Materials and methods

2.1. Preparation of oxygen carriers

The preparation of oxygen carriers is similar to our previous studies [23]. The analytical $CaSO_4$ (Tianjin Fuchen Chemical Factory) and the analytical CuO (Guangdong Guanghua Science and Technology CO., Ltd.) particles were used in this work. $CaSO_4$ was dried at 170°C for 12 h and CuO was dried at 80°C for 12 h. The dried $CaSO_4$ is pressed to tablets under a pressure of 5 Mpa for 10 min and then crushed and sieved to particles with a particle size range of 80–100 mesh. The dried CuO is pressed to tablets under a pressure of 15 Mpa for 10 min and then crushed and sieved to particles with a particle size range of 80–100 mesh. Finally, the $CaSO_4$-based oxygen carrier and CuO-based additive mixed mechanically in various proportions and were ready for experiments.

2.2. Experimental setup

The experiment was carried out using a $CaSO_4$-CuO as an oxygen carrier in a laboratory fixed bed reactor at atmospheric pressure. This is similar to our previous work [25]. Figure 2 shows a schematic of the experimental setup. It mainly comprises a gas feeding system, a reactor, an electric heater, a cooler, and a gas analysis system.

The reactor is a cylindrical fused-silica tube with inside diameter of 13 mm and the length of 600 mm. The OC particles were placed in the middle area while quartz sand was loaded on both sides to reduce the residence time of the gas in the reactor. The temperature was measured with a K-omega thermocouple. The flow rates of reaction gas and calibration gas (CO, CO_2, O_2 and N_2) provided by Shanghai Weichuang Gas Co., Ltd. were all measured by mass flow controllers (MFC, Beijing Seven Star Huachuang Electronics Co., Ltd.). A water cooler was used to cool the hot gas stream from the tubular reactor. The exit gas from the cooler was sampled by syringes for analysis.

The exit gas was diluted by N_2 before measurement. Then, it was analyzed by an infrared flue gas analyzer (York MGA5) to detect SO_2 and O_2. The oxygen carriers after reduction test were characterized by an X-ray diffractometer (XRD, Rigaku Mini Flex 600) and a scanning electron microscope and Energy Dispersive Spectroscope (SEM-EDS, NOVA NANOSEM 450).

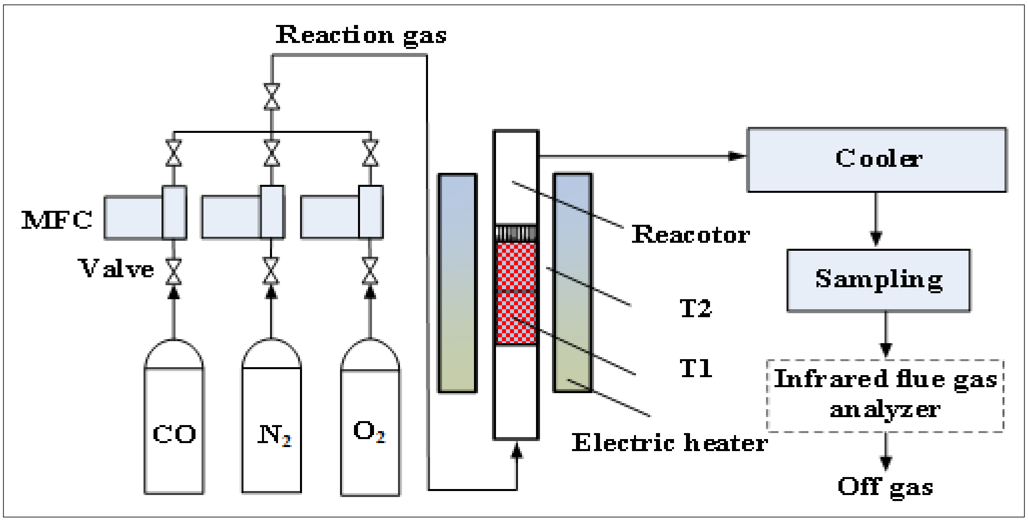

Figure 2. Schematic diagram of the experimental setup

2.3. Experimental procedure

The oxygen carrier reduction was also designed similarly to our previous work [25]. Details as below. A sample of the $CaSO_4$-CuO or $CaSO_4$ was put in the reactor. In N_2 atmosphere, it was then heated to the desired reaction temperature. After the temperature has stabilized at the desired temperature, the nitrogen was switched to a gaseous reactant. Soon afterwards, a gaseous reactant was introduced and the experiment was started. When the reaction was complete, the gaseous reactants were switched to a nitrogen purge and the heater is turned off. When the oxygen carrier particles were cooled to room temperature, they were collected and stored for analysis. Table 1 shows the operation conditions concerning the oxygen carrier reduction.

Table 1. Experimental Conditions Concerning combined Oxygen Carrier Reduction

oxygen carrier	analytical reagent $CaSO_4$ and CuO partiles
sample 1 (CuO/$CaSO_4$ oxygen-carrying ratio=0)	$CaSO_4$ 1000 mg
sample 2 (CuO/$CaSO_4$ oxygen-carrying ratio=5%)	$CaSO_4$ 950 mg + CuO 117.5 mg
sample 3 (CuO/$CaSO_4$ oxygen-carrying ratio=10%)	$CaSO_4$ 900 mg + CuO 235 mg
sample 4 (CuO/$CaSO_4$ oxygen-carrying ratio=15%)	$CaSO_4$ 850 mg + CuO 352.6 mg
sample 5 (CuO/$CaSO_4$ oxygen-carrying ratio=20%)	$CaSO_4$ 800 mg + CuO 470 mg
sample 6 (CuO/$CaSO_4$ oxygen-carrying ratio=50%)	$CaSO_4$ 500 mg + CuO 1175.2 mg
sample 7 (CuO/$CaSO_4$ oxygen-carrying ratio=100%)	CuO 2350.3 mg
pressure (atm)	1
reaction temperature (ºC)	750 - 950
particle size (mesh)	80 - 100
reaction time (min)	60 - 120
reduction gas	5% CO
inert gas	99.999% N_2
gas flow rate(ml/min)	200

2.4. Date evaluation

Both the CO_2 yield η_{CO_2} and the evolution rate of gas product r_i were introduced to facilitate the discussion on CO_2 generating and other gas emissions, and are calculated as follows:

$$r_i = \frac{N_{i,out,t}}{\Delta t \times N_{C,Fuel}} \left(i = CO_2,\ \mathrm{CO},\ \mathrm{SO_2}\right) \qquad (R7)$$

$$\eta_{CO_2} = \frac{\sum_{t=0}^{T} N_{CO_2,out,t}}{N_{C,Fuel}} \qquad (R8)$$

$N_{i,out,t}$ is the molar amount of i product gas species, within the time interval Δt in the gas bags, whereas $N_{C,Fuel}$ is the total molar amount of carbon added in the reactor. The cumulative amount of gas product is the integral of the evolution rate.

3. Results and discussions

3.1. Reaction of $CaSO_4$ and CO

3.1.1. Effects of $CaSO_4$ oxygen carrier mass

The effects of $CaSO_4$ oxygen carrier mass on CO_2 generating and evolutions of SO_2 during the reaction process are shown in Figure 3. The reactions were carried out with 5% CO concentration at 900 °C. As the mass of the oxygen carrier increased, the concentration of CO in the tail gas produced by the reaction decreased and the concentration of CO_2 also increased. However, when the mass of the $CaSO_4$ oxygen carrier was 1000 mg and 1200 mg, the CO_2 concentration did not change much. This may be due to the fact that when the mass of the oxygen carrier was 1000 mg, the lattice oxygen provided was sufficient to react with CO to form CO_2. When the mass of the oxygen carrier was 1000mg, the CO_2 yield was the highest, up to 9.2. SO_2 released rose remarkably with rising the mass of the oxygen carrier. It is because the increase in the amount of oxygen carrier promoted the occurrence of side reactions (R4), (R5) and (R6). The following study was centered on 1000mg $CaSO_4$ with respect to CO_2 generation and gas sulfide releases.

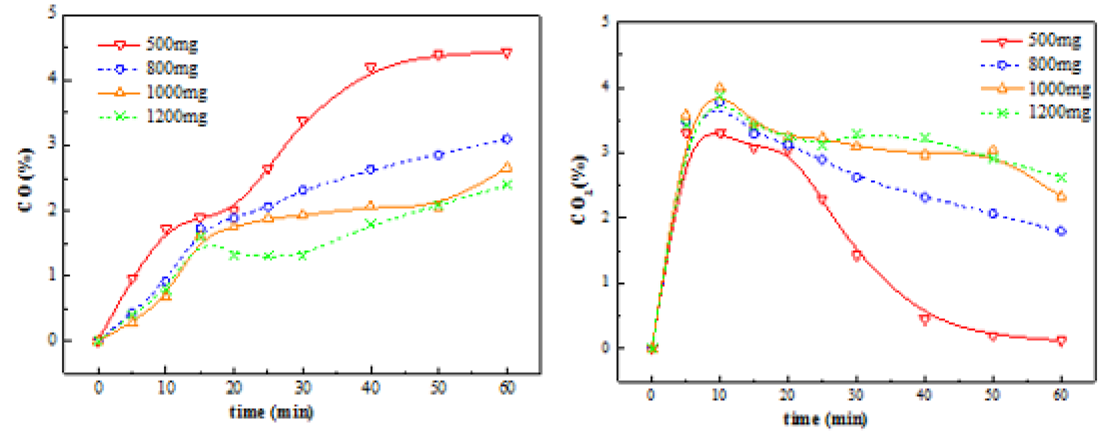

(a)CO concentration (b)CO_2 concentration

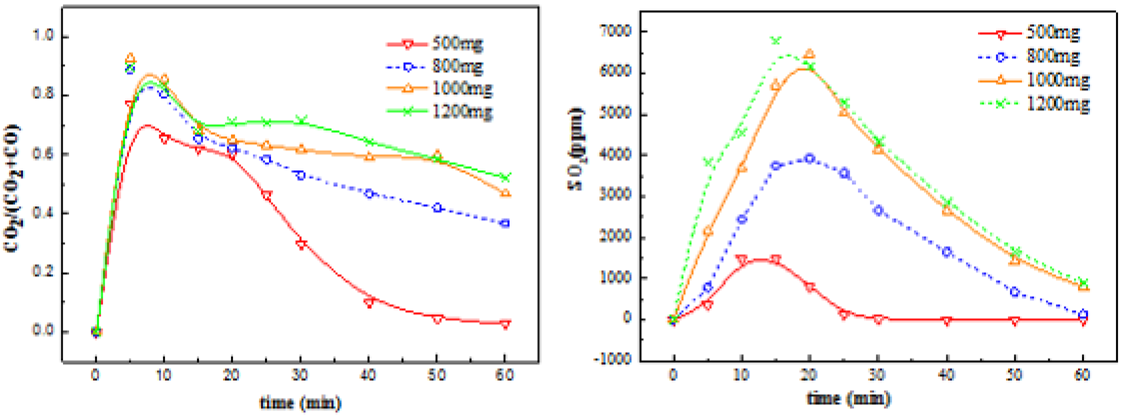

(c)CO_2/(CO_2+CO) (d)SO_2 release

Figure 3. Gas products distributions variation with oxygen carrier mass for $CaSO_4$ reduction by 5% CO concentration at 900°C

3.1.2 Effects of reaction temperature

The effects of reaction temperature on CO_2 generating and evolutions of SO_2 during the reaction process are shown in Figure 4. The reactions were carried out with 5% CO concentration and with $CaSO_4$ oxygen carrier mass of 1000mg. As the reaction temperature increased, the CO_2 production first increased significantly and then decreased slightly. The decrease in CO_2 generation at 950°C is attributed to the thermodynamic limitations of $CaSO_4$ reduction. The release of SO_2 increased remarkably with the increase of reaction temperature. It is due to the increase in temperature, which promotes the occurrence of competitive side reactions and increases the amount of sulfide released. Considering the CO_2 yield and the release of SO_2, the following study was centered on 900°C.

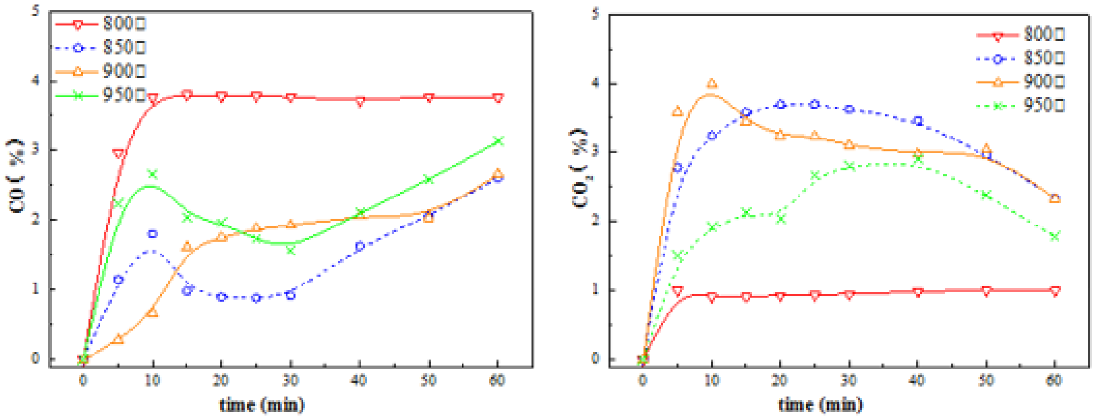

(a)CO concentration (b)CO_2 concentration

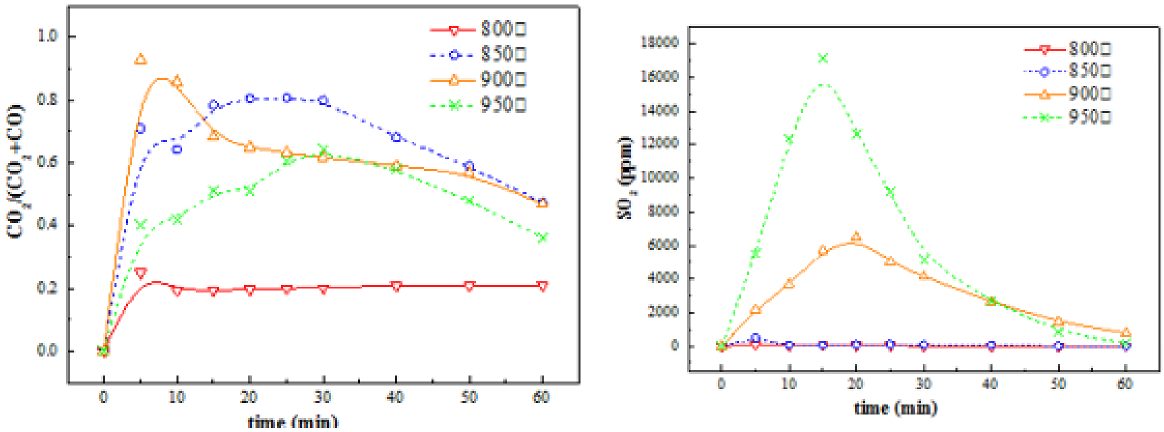

(c)CO_2/(CO_2+CO) (d)SO_2 release

Figure 4. Gas products distributions variation with reaction temperature for $CaSO_4$ reduction by 5% CO concentration

3.2. Reaction of CuO and CO

3.2.1. Effects of Reaction Temperature

The effects of reaction temperature on CO_2 generating during the reaction process are shown in Figure 5. The reactions were carried out with 5% CO concentration and with CuO oxygen carrier mass of 2350.3 mg.

When the reduction reaction temperature was lower than 850°C, the CO concentration in the exhaust gas does not change significantly with the increase of the reduction temperature. When the temperature was raised to 900°C, the CO concentration in the flue gas was significantly higher than that in other reaction temperatures. As the reaction temperature increased, the CuO oxygen carrier occurred sintering in the high-temperature reaction environment, which hindered the reaction between CO and CuO, thereby increasing the concentration of CO. This also led to a low CO_2 yield.

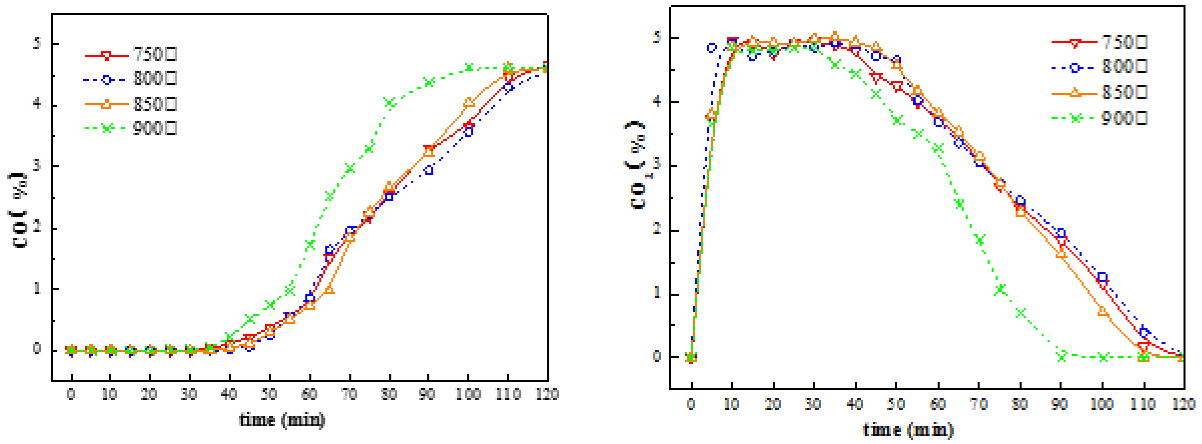

(a)CO concentration

(b)CO_2 concentration

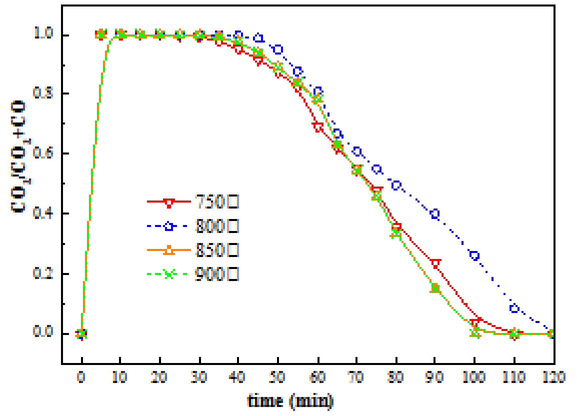

(c)CO_2/(CO_2+CO)

Figure 5. Gas products distributions variation with reaction temperatures for CuO reduction by 5% CO concentration

3.3. Reaction of $CaSO_4$-CuO combined oxygen carrier and CO

3.3.1. Effects of the Oxygen-Carrying Ratios

The effects of the oxygen carrying ratios of CuO to $CaSO_4$ on the evolutions of CO_2 and SO_2 during reaction processes are shown in Figure 6. The reactions were carried out with 5% CO concentration at 900°C. Table 2 shows time required for complete reaction of CuO at different the oxygen carrying ratio of CuO to $CaSO_4$. CuO additive evidently enhanced CO_2 yield. With the increase of the oxygen carrying ratio of CuO to $CaSO_4$, less SO_2 released decreased. On the one hand, the mass of $CaSO_4$ carrier decreased, and the amount of SO_2 released decreasesd. On the other hand, the addition of CuO increased the selectivity of $CaSO_4$ to CaS conversion and the reduction performance of the oxygen carrier decreased, thereby reducing the release of sulfide. Table 3 shows Conversion rate of $CaSO_4$ to CaO and CaS at different the oxygen carrying ratio of CuO to $CaSO_4$. With the increase of the oxygen carrying ratio of CuO to $CaSO_4$, the conversion rate of $CaSO_4$ to CaO decreased, indicating that CuO additive reduced the selectivity of competitive side reactions, thereby reducing the release of sulfides and the deactivation of oxygen carriers. The following experimental study was carried out at the oxygen carrying ratio of CuO to $CaSO_4$ of 20%.

Table 2. Time required for complete reaction of CuO at different the oxygen carrying ratio of CuO to $CaSO_4$

The oxygen carrying ratio of CuO to $CaSO_4$	Time required to generate Cu_2O/min	Time required to generate Cu /min
0%	0	0
5%	1.67	3.33
10%	3.29	6.58
15%	4.90	9.80
20%	6.58	13.16
50%	16.45	32.90
100%	32.9	65.8

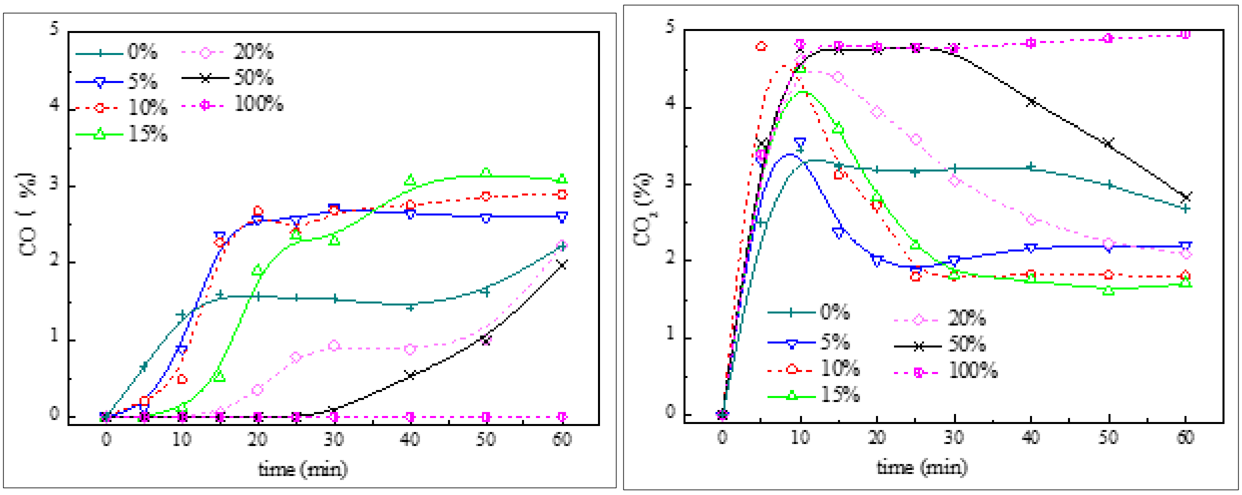

(a)CO concentration (b)CO_2 concentration

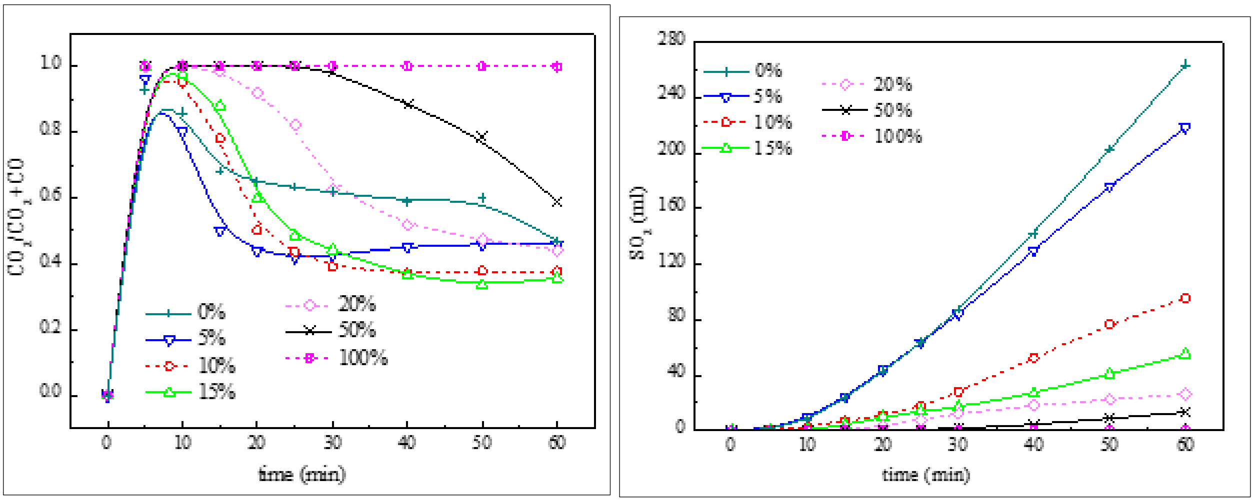

(c)CO_2/(CO_2+CO) (d)SO_2 concentration

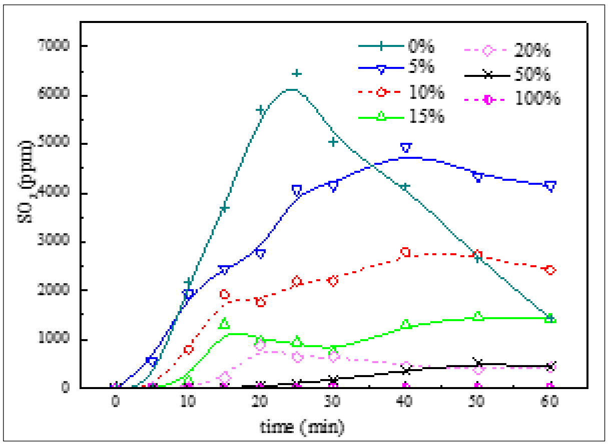

(e)SO_2 release

Figure 6. Gas products distributions variation with oxygen carrying ratios of CuO to $CaSO_4$ for the combined oxygen carrier reduction by 5% CO concentration at 900°C

Table 3. Conversion rate of $CaSO_4$ to CaO and CaS at different the oxygen-carrying ratio of CuO to $CaSO_4$

The oxygen-carrying ratio of CuO to $CaSO_4$	Conversion rate of $CaSO_4$ to CaO	Conversion rate of $CaSO_4$ to CaS
0%	0.250084453	0.357933184
5%	0.207033734	0.296134248
10%	0.096304514	0.292408464
15%	0.05659807	0.407922633
20%	0.03076291	0.559474312
50%	0.020252313	0.56972393

3.3.2. Effects of Reduction Temperature

The effects of reduction temperature on the reaction performance of combined oxygen carrier $CaSO_4$-CuO with the oxygen carrying ratio of 20% are shown in Figure 7. The reactions were carried out with 5% CO concentration and with $CaSO_4$ oxygen carrier mass of 800mg and CuO additive mass of 470mg. Within the reaction temperature of 750 - 900°C, as the temperature of the reduction reaction increased, the concentration of CO gradually decreased, and the yield of CO_2 gradually increased. With the increase of the temperature of reaction, more SO_2 released. It is because as the temperature of the reduction reaction increased, the selectivity of the competitive side reaction increased, resulting in more SO_2 released

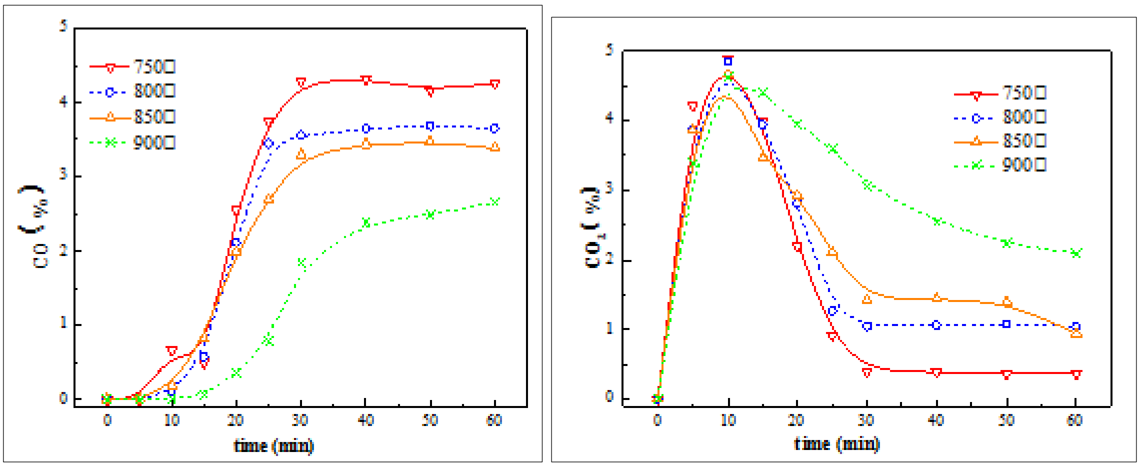

(a)CO concentration

(b)CO_2 concentration

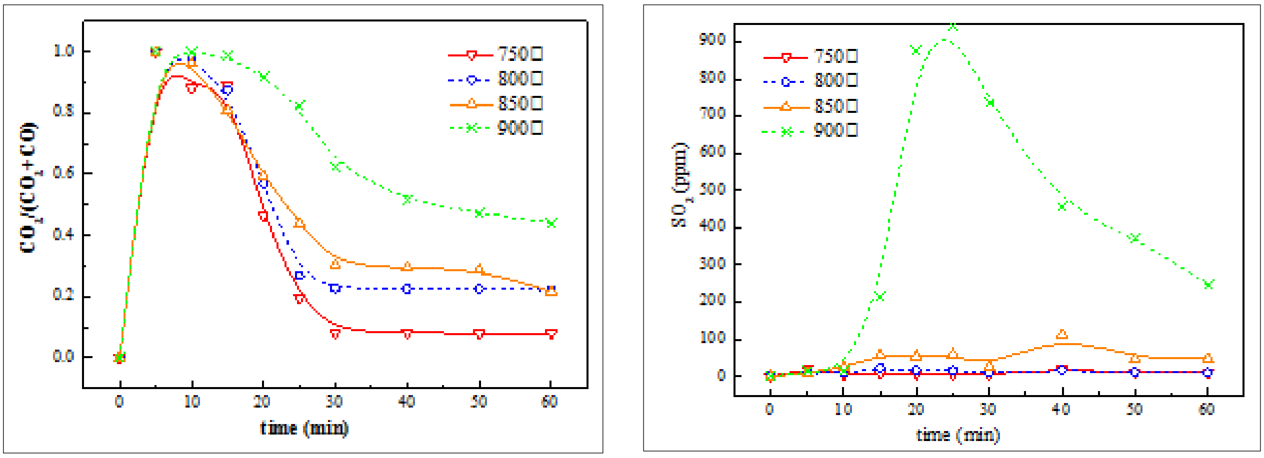

(c)CO_2/(CO_2+CO) (d)SO_2 concentration

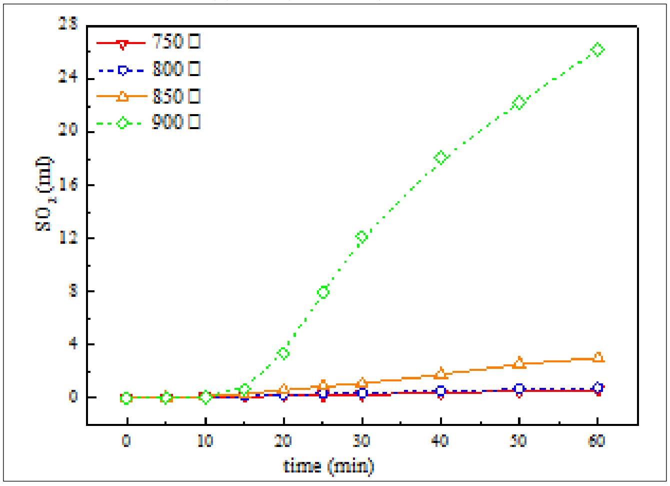

(e)SO_2 release

Figure 7. Gas products distributions variation with reaction temperature for the combined oxygen carrier(CuO/$CaSO_4$ oxygen-carrying ratio is 20%) reduction by 5% CO concentration

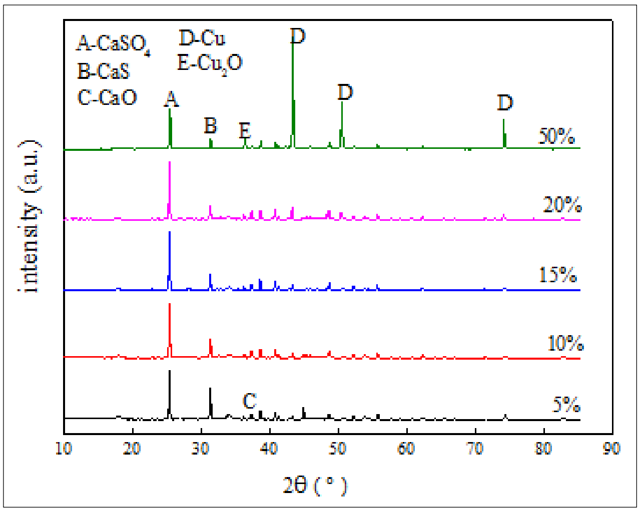

Figure 8. X–ray diffraction (XRD) spectra of reacted $CaSO_4$ and CuO particles (after reaction at 900 °C under 5% CO atmosphere and different oxygen-carrying ratio)

3.4. Characterization and analysis of oxygen carriers

Solid residual was selected for X-ray diffraction analysis. The XRD diagram of the oxygen carrier with different oxygen carrying ratio after reduction are respectively shown in Figure 8. The solid products after the reduction of the combined oxygen carrier $CaSO_4$-CuO mainly contained CaS, CaO, CuO, Cu_2O and $CaSO_4$ which did not participate in the reaction, and no Cu sulfide was detected. In addition, there were Cu_2O and elemental Cu in the product, but no CuO and other copper compounds were found. This indicates that CuO was completely reduced to Cu_2O and Cu, and does not react with other substances.

The particles of the $CaSO_4$-CuO combined oxygen carriers after reactions were analyzed by SEM-EDS. Figure 9 shows the scanning electron micrograph of the combined oxygen carrier reduction reaction under different the oxygen carrying ratio of CuO to $CaSO_4$. Figure 9(a), (b), (c) and (d) shows scanning electron micrographs of $CaSO_4$-CuO oxygen carrying ratios of 0%, 10%, 20%, and 50% combined oxygen carriers, respectively. As shown in Figure 9(a), the surface consists of particles of similar size. The particle distribution is not uniform, and there are some agglomerates of particles. As shown in Figure 9(b), the particle distribution is relatively uniform and the surface of the oxygen carrier is loose and porous. The particle size distribution of the oxygen carrier shown in Figure 9(c) is uneven, and the particle size tends to become larger than those of 9(a) and 9(b). No sintering phenomenon is observed in the particles. 9(d) shows a sintering phenomenon on the surface of the oxygen carrier, resulting in a smaller specific surface area of the oxygen carrier particles, which may be due to sintering of CuO at a high temperature.

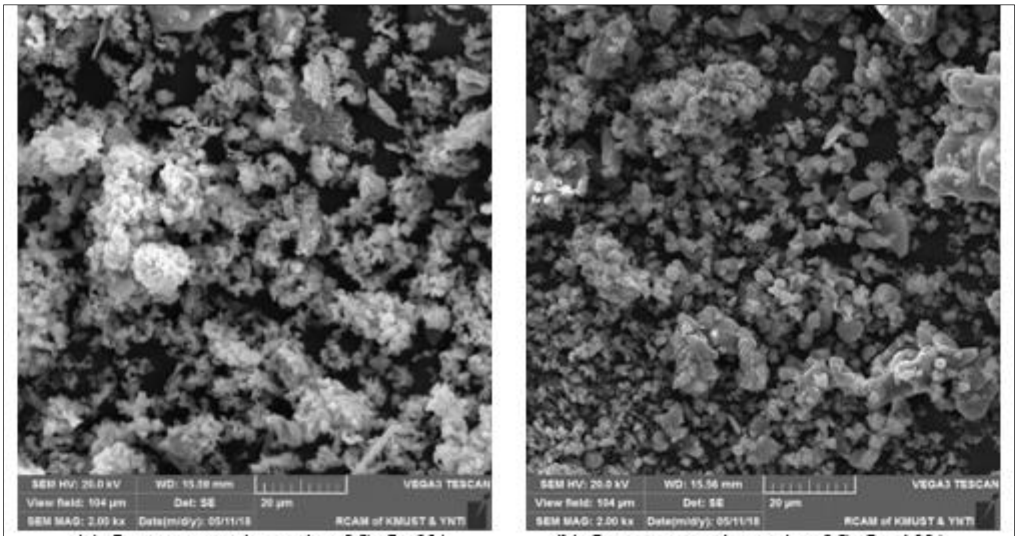

(a) Oxygen-carrying ratio of CuO=0% (b) Oxygen-carrying ratio of CuO =10%

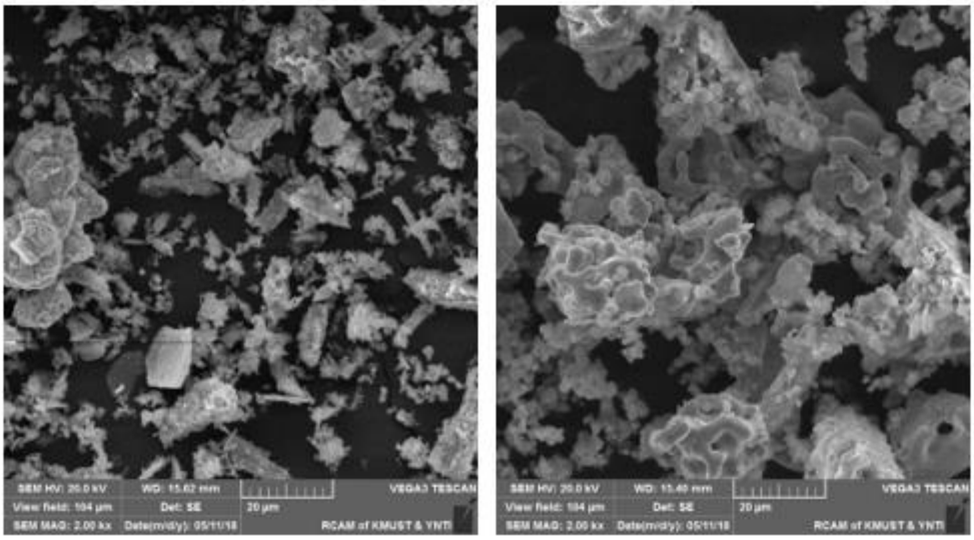

(c) Oxygen-carrying ratio of CuO =20% (d) Oxygen-carrying ratio of CuO =50%

Figure 9. Scanning electron microscope (SEM) spectra of the reduction reaction of combined oxygen carrier at different oxygen carrying ratios of CuO to $CaSO_4$

Table 4. Structure of sample particles after reaction at different the oxygen carrying ratio of CuO to $CaSO_4$

The oxygen carrying ratio of CuO to $CaSO_4$	Specific surface area m^2/g	Total pore volume (cm^3/g)	Average aperture (nm)
0%	11.372	1.609e-02	1.09721e+01
10%	17.750	2.592e-02	5.84168e+00
20%	12.763	1.753e-02	5.49547e+00
50%	3.506	5.624e-03	6.41559e+00

The sample particles after the reaction of the combined oxygen carrier at different oxygen carrying ratio were analyzed by nitrogen adsorption method, and the changes of specific surface area, total pore volume and average pore diameter of the sample were obtained, as shown in Table 4. After the addition of CuO, the specific surface area, total pore volume and average pore diameter of the oxygen carrier increased. Due to the high activity of CuO, the produced CO_2 left more pores on the surface of the particles, and the micropores and micropores aggregate to form mesopores. When the amount of CuO continues to increase, the specific surface area and the total pore volume decreased, and the average pore diameter increased, which was caused by the sintering phenomenon of the oxygen carrier. This is consistent with the phenomenon observed in Figure 9.

Acknowledgement: This work was supported by the National Natural Science Foundation of China (No. 51866003), Yunnan Basic Research Program Project (2019FB071) and China Scholarship Council (No. 201808530023) and Yunnan Province's 10000-Person Plan-Special Project for Young Top Talents (No. YNWR-QNBJ-2019-209).

4. Conclusions

$CaSO_4$-CuO reduction by CO have been investigated in the present work. Chemical looping combustion experiments of CO were carried out by fixed-bed reactor, Gas Chromatograph and Flue Gas Analyzer for quantitive analysis. The effects of oxygen carrier mass (500-1200 mg), reaction temperature (800 - 950 ^oC), CuO/$CaSO_4$ oxygen carrying ratio (0-100%) on sulfur migration and CO_2 generation were discussed. XRD, SEM-EDS, BET and gas analyses were performed to investigate the variations of solid phase change, microscopic morphology and sulfur release with reaction time. Some results are achieved as follows:

- when the mass of $CaSO_4$ carrier is 1000 mg, the reduction performance of $CaSO_4$ carrier is better than that of other masses;
- the addition of CuO additive promotes the reduction reaction of $CaSO_4$, improves the conversion rate of CO, and has a certain inhibitory effect on the release of sulfide. This is mainly because CuO additive reduces the selectivity of competitive side reactions;
- with the increase of oxygen-carrying ratio of CuO, the reduction performance of combined oxygen carrier is enhanced. When the oxygen-carrying ratio is 20%, the reduction performance of combined oxygen carrier increases greatly;
- in the experiment of different reduction reaction temperature when CuO/$CaSO_4$ oxygen-carrying ratio is 20%, the reduction reaction performance of combined oxygen carrier is enhanced with the increase of reduction reaction temperature.

In summary, the addition of the CuO additive increases the reactivity of the calcium-based oxygen carrier while suppressing the release of the sulfurized gas.

Refernces

1. ADANEZ J.; ABAD A.; GARCIA-LABIANO F.; GAYAN P.; DE DIEGO L. F. Prog. Energ. Combust. 2012, 38(2), 215-282.

2. RICHTER H. J.; KNOCHE K. F. ACS Symp. Ser. 1983, 235, 71-86.
3.HOSSAIN M.M., DE LASA H.I. Chemical-looping combustion CLC) for inherent CO_2 separations-a review[J]. Chem. En. Sci., 2008, 63(181): 4433-4451.
4. HAMERS H.P., GALLUCCI F., WILLIAMS G., ANNALAND M.V., Experimental Demonstration of CLC and the Pressure Effect in Packed Bed Reactors Using NIO/CaAl2O4 as Oxygen Carrier[J], Energy & Fuels, 2015, **159**, 828-836
5. A. ABAD, T. MATTISSON, A. LYNGFELT, M. JOHANSSON. Using continuous and pulse experiments to compare two promising nickel-based oxygen carriers for use in chemical-looping technologies[J]. Fuel, 2007, 86, 1021–1035.
6. LAIHONG SHEN, JIAHUA WU, ZHENGPING GAO, JUN XIAO. Reactivity deterioration of $NiO/A1_2O_3$ oxygen carrier for chemical looping combustion of coal in a 10kW/h reactor[J]. Combustion and Flame, 2009, 156, 1377–1385.
7. CARL LINDERHOLM, MATTHIAS SCHMITZ. Chemical-looping combustion of solid fuels in a 100kW dual circulating fluidized bed system using iron ore as oxygen carrier[J]. Journal of Environmental Chemical Engineering, 2016, 4 1029–1039.
8. AURORA RUBEL, KUNLEI LIU, JIM NEATHERY, DARRELL TAULBEE. Oxygen carriers for chemical looping combustion of solid fuels[J]. Fuel, 2009, 88, 876–884.
9. DIPENDU SAHA, RENJU ZACHARIA, LYUBOV LAFI, DANIEL COSSEMENT, RICHARD CHAHINE. Synthesis, characterization and hydrogen adsorption on metal-organic frameworks Al, Cr, Fe and Ga-BTB[J]. Chemical Engineering Journal, 2011, 171, 517–525.
10. VOLKMAR FRICK, MAGNUS RYDÉN, HENRIK LEION. Screening of Combined Mn-Fe-Si Oxygen Carriers for Chemical Looping with Oxygen Uncoupling (CLOU)[J]. Fuel Processing Technology, 2016, 150, 30–40.
11. CAO Y, BIANCA CASENAS A, PAN W P. Redox Reaction Kinetics and Product Characterization with Coal, Biomass, and Solid Waste as Solid Fuels and CuO as an Oxygen Carrier[J]. 2006, 20 (5):1845-1854.
12. TAO SONG, WANJUN GUO, LAIHONG SHEN. Fuel Nitrogen Conversion in Chemical Looping with Oxygen Uncoupling of Coal with a CuO-Based Oxygen Carrier[J]. Energy &Fuels, 2015, 29 (6), 3820−3832.
13. M.M. HOSSAIN, K.E. SEDOR, H.I. DE LASA. $Co–Ni/Al_2O_3$, $Co-Ni/Al_2O_3$ math Container Loading Mathjax oxygen carrier for fluidized bed chemical-looping combustion: Desorption kinetics and metal–support interaction[J]. Chemical Engineering Science, 2007, 62, 5464 – 5472.
14. MEHDI ARJMAND, HENRIK LEION, ANDERS LYNGFELT, TOBIAS MATTISSON. Use of manganese ore in chemical-looping combustion(CLC)-Effect on steam gasification[J]. International Journal of Greenhouse Gas Control, 2012, 8, 56–60.
15. QAMAR ZAFARA, ALBERTO ABAD, TOBIAS MATTISSON, BÖRJE GEVERT, MICHAEL STRAND. Reduction and oxidation kinetics of $Mn_3O_4/Mg–ZrO_2$ oxygen carrier particles for chemical-looping combustion[J]. Chemical Engineering Science, 2007, 62, 6556 – 6567.
16. M. JOHANSSON, T. MATTISSON, A. LYNGFELT. Investigation of Mn_3O_4 with Stabibized ZrO_2 for Chemical-Looping Combustion[J]. Chemical Engineering Research and Design, 2006, 84(A9): 807–818.
17.MATTHIAS SCHMITZ, CARL LINDERHOLM, PETER HALLBERG, SEBASTIAN SUNDQVIST, ANDERS LYNGFELT. Chemical-Looping Combustion of Solid Fuels Using Manganese Ores as Oxygen Carriers[J]. Energy& Fuels, 2016, 30 (2), 1204−1216.
18. SHEN L.; ZHENG M.; XIAO J.; XIAO R. Combust. Flame. 2008, 154(3), 489-506.
19. WANG J.; ANTHONY, E. J. Appl. Energy 2008, 85(2-3), 73-79.
20. MARION J.; BEAL C.; BOUQUET E.; ABDULALLY I.; ANDRUS H. E.; EDBERG C. In: 2nd International oxyfuel combustion conference. 2011, Yeppoon, Australia.
21. ZHENG M.; SHEN L.; FENG X. Energy Convers. Manage. 2014, 83, 270-283.

22. GUO Q.; LIU Y.; JIA W.; YANG M; HU X.; RYU HO-Jung. *Energy Fuels* 2014, 28(11), 7053-7060.
23. MIN ZHENG, SIMEI ZHONG, KONGZHAI LI, HUA WANG, HUILI LIU, YONGGANG WEI, XING ZHU, Characteristics of CaS-CaO Oxidation for Chemical Looping Combustion with a $CaSO_4$-Based Oxygen Carrier[J]. Energy & Fuels, 2017, **31**(12), 13842-13851
24. WANG B.; ZHANG, B.; WANG, W.; ZHAO, H.; ZHENG, C. In: 4th International Conference on Chemical Looping. 2016, Nanjing, China.
25. ZHENG M.; XING Y.; LI K.; ZHONG S.; WANG H.; ZHAO B. Energy Fuels 2017, 31(5), 5255-5265.

Manuscript received: 27.04.2021